



Geophysical Research Letters®

RESEARCH LETTER

10.1029/2024GL108373

The Role of Ocean Mesoscale Variability in Air-Sea CO₂ Exchange: A Global Perspective

Yiming Guo^{1,2}  and Mary-Louise Timmermans^{1,2} 

¹Department of Earth & Planetary Sciences, Yale University, New Haven, CT, USA, ²Yale Center for Natural Carbon Capture, New Haven, CT, USA

Key Points:

- Over 30% of air-sea CO₂ flux variability is attributed to ocean spatial scales smaller than 2° in eddy-rich regions
- The cumulative mesoscale-induced CO₂ flux is on the order of 10⁵ tonnes of carbon per year
- Mesoscale-related CO₂ flux is governed by both relative vorticity and the background gradient of partial pressure of CO₂

Supporting Information:

Supporting Information may be found in the online version of this article.

Correspondence to:

Y. Guo,
yiming.guo@yale.edu

Citation:

Guo, Y., & Timmermans, M.-L. (2024). The role of ocean mesoscale variability in air-sea CO₂ exchange: A global perspective. *Geophysical Research Letters*, 51, e2024GL108373. <https://doi.org/10.1029/2024GL108373>

Received 16 JAN 2024

Accepted 16 APR 2024

Author Contributions:

Conceptualization: Yiming Guo, Mary-Louise Timmermans

Formal analysis: Yiming Guo

Funding acquisition: Mary-Louise Timmermans

Investigation: Yiming Guo, Mary-Louise Timmermans

Methodology: Yiming Guo, Mary-Louise Timmermans

Supervision: Mary-Louise Timmermans

Validation: Yiming Guo

Visualization: Yiming Guo

Writing – original draft: Yiming Guo

Writing – review & editing: Yiming Guo, Mary-Louise Timmermans

© 2024. The Authors.

This is an open access article under the terms of the [Creative Commons Attribution-NonCommercial-NoDerivs License](https://creativecommons.org/licenses/by/4.0/), which permits use and distribution in any medium, provided the original work is properly cited, the use is non-commercial and no modifications or adaptations are made.

Abstract Ocean mesoscale flows significantly influence nutrient distribution and biological productivity, yet the scarcity of eddy-permitting observational data sets and climate modeling hinders understanding their role in carbon sequestration. Using an eddy-resolving global simulation, this study investigates the significance of ocean mesoscales in air-sea carbon dioxide (CO₂) exchange. Results show over 30% of CO₂ flux variance in energetic regions attributed to flows with horizontal scales smaller than 2°. Mesoscale flows can drive a cumulative CO₂ flux that is either a net carbon sink or source depending on region, with magnitudes on the order of 10⁵ tonnes of carbon per year. Variations in this mesoscale-related CO₂ flux are correlated with local relative vorticity and the background gradient of ocean partial pressure of CO₂. This analysis underscores the importance of considering ocean mesoscales in monitoring carbon flux, highlighting the need to explore the influence of increasing eddy activity on carbon uptake in a changing climate.

Plain Language Summary This study investigates the influence of ocean flows with horizontal scales of tens to hundreds of kilometers (called mesoscale flows) on the exchange of carbon dioxide between the ocean and the atmosphere using a state-of-the-art high resolution global simulation. It is shown that in certain parts of the ocean, more than 30% of the variability in carbon dioxide exchange at the ocean surface is linked to these relatively small-scale ocean motions. It is further revealed that mesoscale flows can lead to a significant gain or loss of carbon from the ocean at the regional level, and that depends on how the flow is oriented with respect to the background distribution of carbon in the ocean. Gaining a better understanding of how the mesoscale flow features influence air-sea carbon dioxide exchange is crucial for understanding the ocean's role in the carbon cycle and its ability to absorb and store carbon in a changing climate.

1. Introduction

The ocean acts as an extensive carbon reservoir, mitigating climate change effects by absorbing and storing approximately 26% of anthropogenic carbon dioxide (CO₂) from the atmosphere (Friedlingstein et al., 2023). Globally, the ocean has the capacity to uptake more than 2,000 megatonnes of carbon (MtC, 10⁶ tC) annually through CO₂ flux at the surface (Friedlingstein et al., 2023). This air-sea CO₂ flux exhibits variations across a range of spatial and temporal scales (Gruber et al., 2023), predominantly governed by the difference in partial pressure of CO₂ ($p\text{CO}_2$) between the atmosphere and the ocean (Gu et al., 2023; Mongwe et al., 2018). Notably, high-quality in-situ measurements of CO₂ flux obtained through the eddy covariance method are mostly limited to local scales (Miller et al., 2010, 2024). Previous observation-based studies, such as those utilizing the Surface Ocean CO₂ Atlas (SOCAT) product to assess CO₂ flux variability, have primarily relied on coarse gridded data (Landschützer et al., 2020; Tokoro et al., 2023). Additionally, CO₂ flux variations in climate simulations with low-resolution ocean models exhibit large biases (Mongwe et al., 2018; Wong et al., 2022). Therefore, our current understanding of the natural variability of air-sea CO₂ flux, which largely relies on coarse-resolution data sets and climate models, may potentially lead to an underestimation of the contributions from small-scale variability in the ocean.

As the most energetic features in the ocean, mesoscale phenomena with horizontal spatial scales on the order of 10–100 km, including coherent vortices (eddies), and strong lateral density gradients in the form of fronts and meanders, are ubiquitous in the global ocean (Chelton et al., 2011) and can significantly influence oceanic and atmospheric conditions (e.g., Frenger et al., 2013; Guo et al., 2023). Their pivotal role in redistributing ocean tracers such as mass (Zhang et al., 2014), salt (Melnichenko et al., 2021), and heat (Guo & Bishop, 2022) has been well-established. Recent observational evidence on regional ocean scales suggests that coherent mesoscale eddies

can significantly modify local air-sea CO₂ exchange (e.g., Ford et al., 2023; Kim et al., 2022). However, a consensus has yet to be reached on whether mesoscale eddies with specific polarity and anomalous seawater properties act as a sink of CO₂ to the ocean (Ford et al., 2023; Jones et al., 2017; T. Smith et al., 2023) or a source of CO₂ to the atmosphere (Chen et al., 2007; Kim et al., 2022; Pezzi et al., 2021). This open question underscores the complex and spatially heterogeneous nature of mesoscale influences on carbon dynamics in the global ocean, motivating further study using high-resolution data with improved geographic coverage.

Due to a sparsity of in-situ observations and the computational burden of eddy-resolving (i.e., 1/10° and finer) global simulations, there has been little analysis on how mesoscale processes influence air-sea CO₂ fluxes from a global perspective. Harrison et al. (2018) compare global high-resolution (1/10°) and standard low-resolution (1°) climate simulations, demonstrating that ocean mesoscale variability may increase or decrease carbon export to the deep ocean by as much as 50% at regional scales. More recently, Guo and Timmermans (2024b), utilizing an eddy-resolving global biogeochemical simulation, characterized a strong link between eddy activity and ocean *p*CO₂ changes in mid-latitude regions. This points to the potential involvement of mesoscale processes in driving *p*CO₂ variations, likely modulating carbon flux across a large spatial domain. Ford et al. (2023) found that long lived (>1 year) eddies enhanced CO₂ uptake in the South Atlantic Ocean by 0.08 ± 0.04%. There remain many open questions related to the influence of mesoscale motions on CO₂ fluxes, including whether ocean eddies serve as hotspots for CO₂ sink or source in specific dynamic regions (Jones et al., 2017), whether mesoscale variability can significantly modulate CO₂ fluxes at regional (Ford et al., 2023) and global scales, and whether previous studies that do not resolve the mesoscales underestimate CO₂ flux variations. Here we address certain aspects of these important questions via diagnosing a mesoscale-associated CO₂ flux in a global eddy-resolving simulation.

2. Data and Methods

2.1. Observational-Based Data Sets

We use an observation-based product of sea surface *p*CO₂ and air-sea CO₂ fluxes from 1982 to 2000, which integrates over 10 million data values collected from ship-based measurements, moorings, and drifters (Landschützer et al., 2020). The gridded product is created using a 2-step neural network method described by Landschützer et al. (2016); Jersild et al. (2023). The air-sea CO₂ fluxes are computed from the air-sea *p*CO₂ difference and a bulk gas transfer formulation (Landschützer et al., 2016; Wanninkhof, 2014). This product provides monthly time series of *p*CO₂ and CO₂ flux at a spatial resolution of 1° × 1° covering most of the global ocean. Due to the relatively coarse spatial resolution (not eddy-permitting) of this data set, we only used this product for model evaluation compared to climatology and large-scale temporal variations. Note that there could be biases in the gridded product, particularly in high variance and/or undersampled regions such as coastal areas (Landschützer et al., 2016). However, we use this observation-based product solely for evaluating the model output with respect to overall spatial patterns of CO₂ flux. Our main mesoscale-related analysis is conducted using an eddy-resolving global simulation. Finally, we use climatological mean sea surface height (SSH) from satellite observations from the DUACS multimission altimeter data processing system to indicate the mean pattern of ocean circulation and gyres.

2.2. Eddy-Resolving Global Biogeochemical Simulation

The simulation analyzed here is a global eddy-resolving (with nominal horizontal resolution of 0.1°; Figure S1a in Supporting Information S1) ocean, sea ice, and biogeochemical coupled simulation with 62 vertical levels within the Community Earth System Model (CESM). The ocean model is the Parallel Ocean Program (POP), version 2 (R. Smith et al., 2010), coupled with the Community Ice Code (CICE) version 4 (Hunke et al., 2010). The model is forced by the Japanese 55-year Reanalysis (JRA55) (Kobayashi et al., 2015) from 1958 to 2000. The air-sea CO₂ flux in the model is calculated based on the bulk formula (Persch et al., 2023) with forced atmospheric conditions and simulated *p*CO₂. A detailed description of the ocean configuration is given by Bryan and Bachman (2015); Guo, Bishop, et al. (2022). The ocean biogeochemical model in this simulation uses the prognostic Marine Biogeochemistry Library from CESM (Long et al., 2021). This biogeochemistry-coupled high-resolution POP simulation will be referred as POP-BGC-HR below, which is the same as that used by Guo and Timmermans (2024b). A more detailed description of the model is given by Long et al. (2021); Guo and Timmermans (2024b). Due to computational constraints and the availability of model

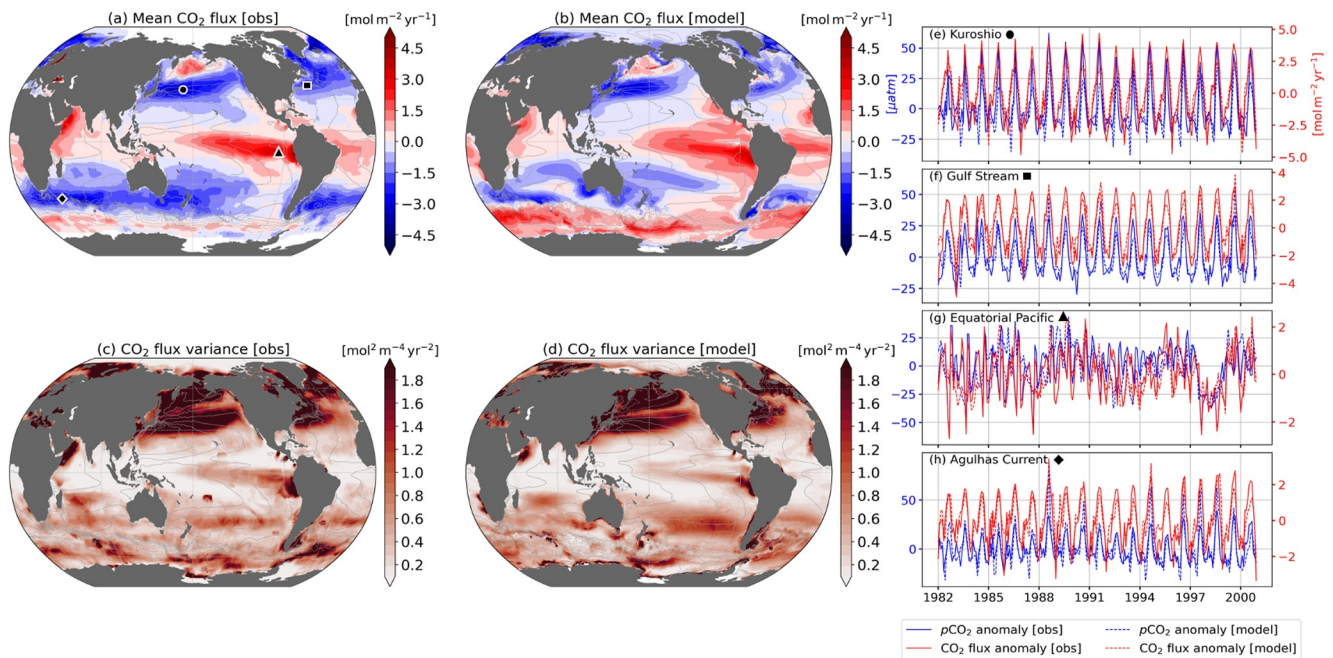


Figure 1. Comparison of climatology and variability of air-sea CO_2 flux between observation-based data set and the model during 1982–2000. (a) Mean CO_2 flux climatology in observation-based data set; (b) Mean CO_2 flux in the model; (c) Total variance of monthly time series of CO_2 flux in observation-based data set; (d) Total variance of monthly time series of CO_2 flux in the model; (e)–(h) Monthly time series of $p\text{CO}_2$ (blue lines) and air-sea CO_2 flux (red lines) anomalies in observation-based data set (solid lines) and model (dashed lines) at four locations as marked in panel (a). Gray contours in each panel are mean sea surface height contours (CI = 20 cm) from satellite altimetry (a, c) and POP-BGC-HR (b, d).

output, we used monthly POP-BGC-HR output from 1982 to 2000 in this study. This temporal frequency does not allow for daily to weekly variability in ocean fields; as such, more persistent mesoscale features (e.g., current meanders) may be better represented compared to features with evolution and translation timescales on the order of days to weeks.

Comparable spatial patterns and magnitudes are observed in both climatology and variability of air-sea CO_2 flux between observation-based data set (Figures 1a and 1c) and POP-BGC-HR (Figures 1b and 1d). The climatology fields are long-term averages spanning the entire data period and the variability is estimated by the total variance of the monthly time series of CO_2 flux. The mean distribution of CO_2 flux (Figures 1a and 1b) shows significant spatial variability in both magnitude and direction, with positive CO_2 flux (a net source of CO_2 to the atmosphere) in tropical and high latitude regions, and negative CO_2 flux (a net sink of CO_2 into the ocean) in mid-latitudes, influenced by regional circulation patterns, ice melt, biological activity, and hydrographic conditions (e.g., Arroyo et al., 2019; Takahashi et al., 2002, 2009; Tozawa et al., 2022). In general, regions with the largest CO_2 flux magnitudes also display the largest variance, particularly in mid and high latitude regions (Figures 1c and 1d), where mesoscale activity is vigorous. We selected four sites in different parts of the global ocean (the Kuroshio, Gulf Stream and Agulhas currents and the Equatorial Pacific, Figure 1a) chosen as they are typical regions where both mesoscale energy and induced transport are strong (following Guo, Bachman, et al., 2022; Martínez-Moreno et al., 2021). CO_2 flux variations at these representative locations within these regions are synchronized with changes in ocean $p\text{CO}_2$ (in both observation-based data set and POP-BGC-HR, Figures 1e–1h), indicating the dominant influence of $p\text{CO}_2$ variations in setting CO_2 flux anomalies (Gu et al., 2023; Mongwe et al., 2018). Positive $p\text{CO}_2$ anomalies induce positive CO_2 fluxes (i.e., a source of CO_2 to the atmosphere), while negative $p\text{CO}_2$ anomalies correspond to negative CO_2 fluxes (i.e., a sink of CO_2 to the ocean). Changes in $p\text{CO}_2$ are induced by surface heating and cooling, upwelling and downwelling, as well as variations in ocean mixing and primary production (Gruber et al., 2023; Guo & Timmermans, 2024b). Since seasonality predominantly governs the temporal variability in $p\text{CO}_2$ and CO_2 flux in most ocean regions (Takahashi et al., 2002), CO_2 flux variance is comparable between the low-resolution observation-based product and the high-resolution model output. However, the coarse resolution observation-based product does not effectively capture the mesoscale variability spatially resolved by POP-BGC-HR.

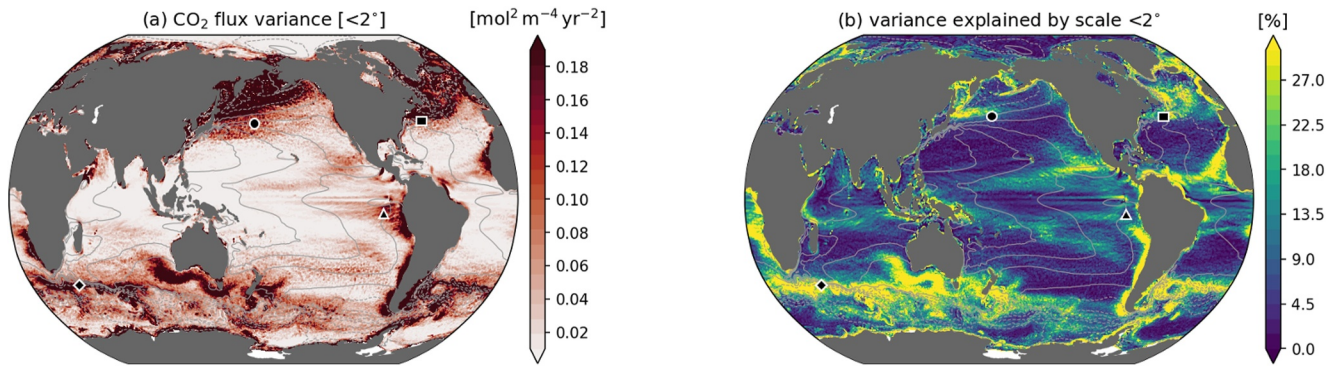


Figure 2. Air-sea CO₂ flux variance explained by the mesoscale. (a) CO₂ flux variance associated with small scales (<nominal 2°); (b) Percentage of CO₂ flux variance explained by small scales. Gray contours are mean sea surface height contours (CI = 20 cm) in the model. Black markers denote the four locations shown in Figure 1.

2.3. Mesoscale Extraction Through a Coarse-Graining Approach

To investigate the effect of mesoscale features on air-sea CO₂ flux in the global ocean, we employ a coarse-graining approach specifically designed for spatial scale separation in oceanographic settings (Storer & Aluie, 2023). This technique has been successfully implemented on scalar and vector oceanic fields in both Cartesian and spherical coordinates (e.g., Aluie et al., 2018). In this study, we use the coarse-grained (or low-pass filtered) field of CO₂ flux to retain only mesoscale flow features from the original fields. The cutoff spatial scale is set at a nominal 2° (ranging from 50 km at high latitudes to 220 km at low latitudes; Figure S1c in Supporting Information S1), considering that both the eddy scale in the real ocean and the theoretical deformation scale in the model (ranging from 20 km at high latitudes to 120 km at low latitudes) are generally smaller than the local 2° cutoff (see Chelton et al., 1998, 2011 and Figure S1a in Supporting Information S1). Ocean models in traditional climate simulations, which have been utilized to diagnose CO₂ flux variability, typically have horizontal resolutions of 1°–2° (Mongwe et al., 2018). The selection of a 2° spatial cutoff in this work additionally aims to evaluate the unresolved variability in CO₂ flux in low-resolution models. Throughout the paper, we refer to the isolated field as the “mesoscale” portion of the total field and denote the mesoscale-related CO₂ flux as $F_{CO_2}^{<2^\circ}$.

3. Results

After coarse-graining, the remaining CO₂ flux associated with mesoscale (<2°) features shows the largest flux variability in mid and high latitude regions (Figure 2a). The percentage of total flux variance that is accounted for by mesoscale variability exhibits strong spatial heterogeneity, with the highest percentage found in eddy-rich regions such as western boundary currents and the Antarctic Circumpolar Current, and the lowest percentage in the subtropical gyres (Figure 2b). More than 30% of the total variance in air-sea CO₂ flux can be attributed to ocean mesoscale variability in these energetic regions. This suggests that resolving mesoscale features may be important for appropriately characterizing natural variability of ocean carbon uptake.

Given that the mesoscale flow field can explain a significant portion of CO₂ flux variance (Figure 2), the next question arises: does mesoscale variability induce a sink of CO₂ to the ocean (Ford et al., 2023) or a source of CO₂ to the atmosphere, and what factors control such a modification to local mean air-sea CO₂ flux? To address this question, we analyze cumulative mesoscale-related CO₂ flux ($F_{CO_2}^{<2^\circ}$) at a range of select locations in the global ocean. This is one avenue for investigation of the net contribution of mesoscale features in general, as opposed to a focus only on coherent mesoscale eddies. We begin by examining the four locations shown in Figure 1. At locations along the Kuroshio Extension and Gulf Stream, time series of $F_{CO_2}^{<2^\circ}$ and the cumulative sum indicate a net CO₂ sink by the oceans induced by mesoscale variability (Figures 3a and 3b). In contrast, the cumulative $F_{CO_2}^{<2^\circ}$ at locations in the equatorial Pacific and Agulhas current suggests that in these ocean regions mesoscale flows are associated with a net CO₂ source to the atmosphere (Figures 3c and 3d). Globally, the linear regressed slopes of the cumulative $F_{CO_2}^{<2^\circ}$ for the period 1982–2000 are estimated within each 2° × 2° grid cell (Figure 3e). Their global distribution shows significant spatial heterogeneity, where the net flux associated with mesoscale flows can be either a carbon source or a sink in different dynamic regions.

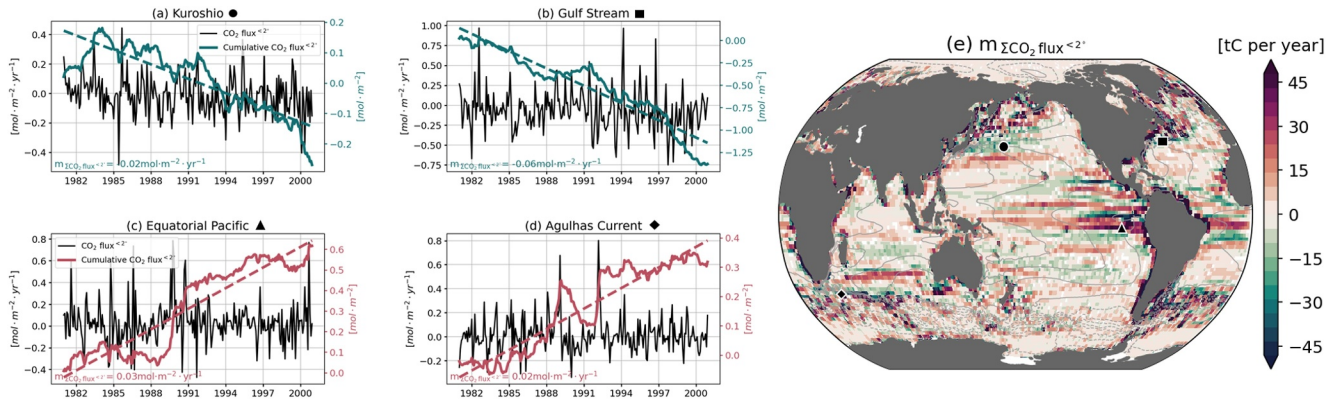


Figure 3. Mesoscale ($< \text{nominal } 2^\circ$) contribution to air-sea CO_2 flux in the model. (a)–(d) Monthly time series of $F_{\text{CO}_2}^{<2^\circ}$ (black lines) and cumulative $F_{\text{CO}_2}^{<2^\circ}$ (green/red solid lines) in four locations marked in Figure 1 and (e). Dashed lines are the least squares regression of cumulative flux for the period 1982–2000; slopes are indicated in the bottom left; (e) Global distribution of regressed slopes of cumulative $F_{\text{CO}_2}^{<2^\circ}$. Units are converted from $\text{mol} \cdot \text{m}^{-2}$ per year to tonnes of carbon per year using the atomic mass of carbon. Green colors imply a CO_2 sink and red colors, a source. Slopes that are not statistically significant (90% confidence level) are masked by white dots. Contours represent mean sea surface height contours (CI = 20 cm) in the model.

The overall spatial pattern tends to exhibit a zonal alternation between net sources and sinks in many parts of the global ocean with an active mesoscale flow field (Figure 2a). Specific regions can indicate contiguous patterns that show either a net CO_2 source or sink. For example, a carbon sink area is observed along the Kuroshio Extension and a source area is identified south of the Kuroshio (Figure 3e). Even though mesoscale activity is responsible for significant variance in CO_2 flux in these regions, the time-integrated cumulative (net) effect remains only a small percentage of the regional total. In the Kuroshio region, for example, where there is net CO_2 uptake by the oceans, 14% of the variance can be attributed to the mesoscale (Figure 2b). However, mesoscale flows here are associated with only 0.06% of the total CO_2 accumulation in the region (i.e., net uptake on the order of 0.5 MtC per year). On a global scale, the zonally integrated cumulative $F_{\text{CO}_2}^{<2^\circ}$ yields a net carbon uptake from mesoscale variability amounting to 0.72 MtC per year.

As two representative examples of eddy-rich regions, we select the Gulf Stream and the Agulhas current to further illustrate the regional carbon flux induced by mesoscale processes and explore its relationship with local dynamics. We find that the cumulative $F_{\text{CO}_2}^{<2^\circ}$ exhibits approximately zonal bands alternating in the meridional direction between positive (a source) and negative (a sink) flux anomalies along frontal zones (Figures 4a and 4e). These spatial characteristics in cumulative $F_{\text{CO}_2}^{<2^\circ}$ are linked to relative vorticity ζ (Figures 4b and 4f; see definition

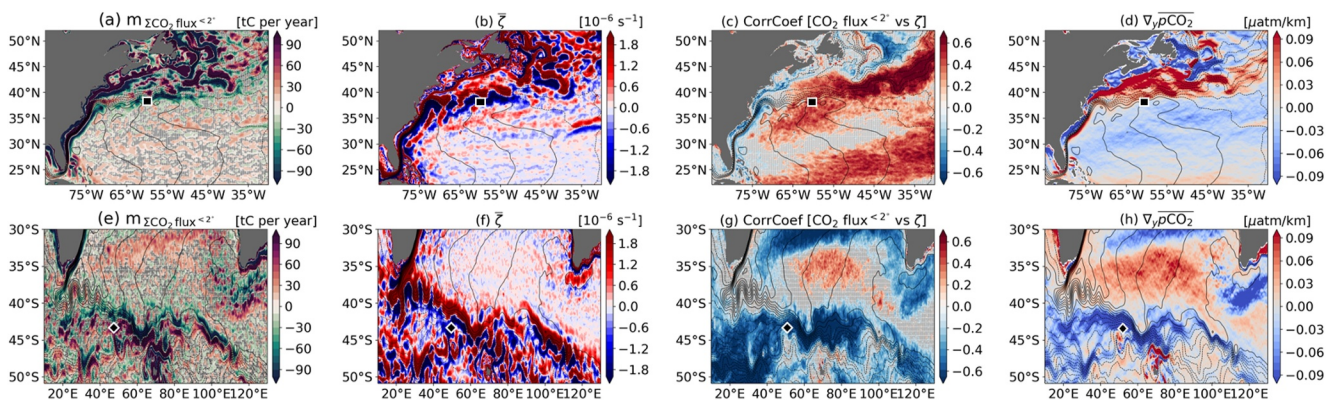


Figure 4. (a) Spatial distribution of regressed slopes of cumulative mesoscale-related CO_2 flux in the Gulf Stream region (gray hatched areas denote regressed slopes below the 90% confidence level); (b) Mean distribution of relative vorticity; (c) Distribution of correlation coefficients between monthly series of mesoscale air-sea CO_2 flux and relative vorticity (gray hatched areas denote correlations below the 90% confidence level); (d) Mean pattern of cross-stream $p\text{CO}_2$ gradient. (e)–(h) same as (a)–(d) but for the Agulhas current. Gray contours represent mean sea surface height contours. (CI = 20 cm) in the model. Black markers denote the two locations in Figures 3b and 3d.

of ζ in Supporting Information S1). Positive relative vorticity indicates counterclockwise flow (i.e., termed cyclonic (anticyclonic) in the northern (southern) hemisphere), while negative vorticity indicates clockwise flow (i.e., anticyclonic (cyclonic) in the northern (southern) hemisphere). Although the spatial distributions of both ζ and $F_{\text{CO}_2}^{<2^\circ}$ are noisy, their correlation scales are high and display significant spatial coherence (Figures 4c and 4g), indicating an influence of relative vorticity on $F_{\text{CO}_2}^{<2^\circ}$ that holds at larger scales. In the Gulf Stream, in general, relative vorticity is positively correlated with $F_{\text{CO}_2}^{<2^\circ}$, which suggests that positive relative vorticity likely increases CO_2 levels in the ocean there, leading to CO_2 releasing to the atmosphere. Conversely, negative relative vorticity is correlated with lower ocean CO_2 levels, leading to a CO_2 sink to the region. In contrast to the Gulf Stream, the $F_{\text{CO}_2}^{<2^\circ} - \zeta$ correlation in the Agulhas current is predominantly negative, particularly in the frontal areas. In such regions, a positive relative vorticity is associated with negative $F_{\text{CO}_2}^{<2^\circ}$ (a sink), and negative relative vorticity with a CO_2 source (Figures 4e, 4f, and 4g). The strength and sign of these differing correlations in different regions are related to the background cross-stream $p\text{CO}_2$ gradient. The cross-stream $p\text{CO}_2$ gradient, generally oriented along the meridional direction, is calculated within stream coordinates based on the mean surface current. The broad positive $F_{\text{CO}_2}^{<2^\circ} - \zeta$ correlation in the Gulf Stream is linked to a strong northward increase in $p\text{CO}_2$ (Figure 4d). Similarly, a negative cross-stream $p\text{CO}_2$ gradient (i.e., a southward increase of $p\text{CO}_2$) corresponds to the negative $F_{\text{CO}_2}^{<2^\circ} - \zeta$ correlation along the Agulhas current (Figure 4h).

This finding clarifies the different behavior observed in cumulative fluxes at the four representative locations in Figures 3a–3d. Whether mesoscale-related net CO_2 flux acts as a local carbon sink (Figures 3a and 3b) or source (Figures 3c and 3d) largely depends on the local background cross-stream $p\text{CO}_2$ gradient and $F_{\text{CO}_2}^{<2^\circ} - \zeta$ correlation. For example, for the location along the Gulf Stream (Figure 3b), the observed net carbon sink associated with mesoscale variability is linked to negative relative vorticity and positive cross-stream $p\text{CO}_2$ gradient (marker in Figures 4b and 4d), suggesting that clockwise-rotating water parcels bring low $p\text{CO}_2$ water to this location and induce a sink of CO_2 to the ocean. The positive $F_{\text{CO}_2}^{<2^\circ} - \zeta$ correlation (marker in Figure 4c) also indicates the in-phase connection between cumulative mesoscale-related flux and relative vorticity at this location. Conversely, at the location near the Agulhas current, the mesoscale-related CO_2 source coincides with a negative relative vorticity, a negative cross-stream gradient, and a negative $F_{\text{CO}_2}^{<2^\circ} - \zeta$ correlation (marker in Figures 4e–4h). Note how current meandering leads to adjacent bands of net source and sink (Figures 4a and 4e), which are linked to the banded distribution of relative vorticity (Figures 4b and 4f).

The strong connection between the local cross-stream $p\text{CO}_2$ gradient and the local $F_{\text{CO}_2}^{<2^\circ} - \zeta$ correlation is evident at a global scale (Figure 5), where a positive correlation generally aligns with a positive cross-stream $p\text{CO}_2$ gradient in eddy-rich regions (black boxes in Figures 5a and 5b), and vice versa. When a positive cross-stream $p\text{CO}_2$ gradient is present (Figure 5c), as observed in regions such as the Kuroshio Extension and Gulf Stream, mesoscale motions with negative relative vorticity tend to give rise to a local $p\text{CO}_2$ deficit leading to a CO_2 sink, and positive relative vorticity corresponds to a source of CO_2 to the atmosphere (i.e., a positive $F_{\text{CO}_2}^{<2^\circ} - \zeta$ correlation). Conversely, when a negative cross-stream $p\text{CO}_2$ gradient is present (Figure 5d), as generally observed in the region of the Agulhas current, the negative $F_{\text{CO}_2}^{<2^\circ} - \zeta$ correlation suggests that negative relative vorticity contributes to CO_2 release and positive relative vorticity corresponds to a sink of CO_2 to the oceans. In brief, mesoscale motions can stir and transport water with anomalous properties in the context of the background $p\text{CO}_2$ gradient, inducing local CO_2 flux anomalies that depend on the sign (vorticity) of these rotational motions.

4. Summary and Discussion

The emerging regional observational evidence regarding the influence of mesoscale eddies on air-sea CO_2 exchange underscores the necessity for in-depth investigations into their global effects. It also raises questions on the limitations of using low-resolution climate models that do not resolve mesoscale features to study CO_2 flux variability. In this work, we investigate the contribution of ocean mesoscale variability to air-sea CO_2 fluxes from a global perspective by analyzing the CO_2 flux anomaly within the mesoscale band ($<2^\circ$) in a global eddy-resolving biogeochemical simulation. We find that in eddy-rich mid-latitude regions, ocean variability with scales smaller than approximately 200 km can account for over 30% of the total CO_2 flux variability. The cumulative net CO_2 flux associated with mesoscale motions is on the order of 10^5 tC per year. The global pattern of cumulative $F_{\text{CO}_2}^{<2^\circ}$ exhibits significant spatial heterogeneity, with the highest values in western boundary currents,

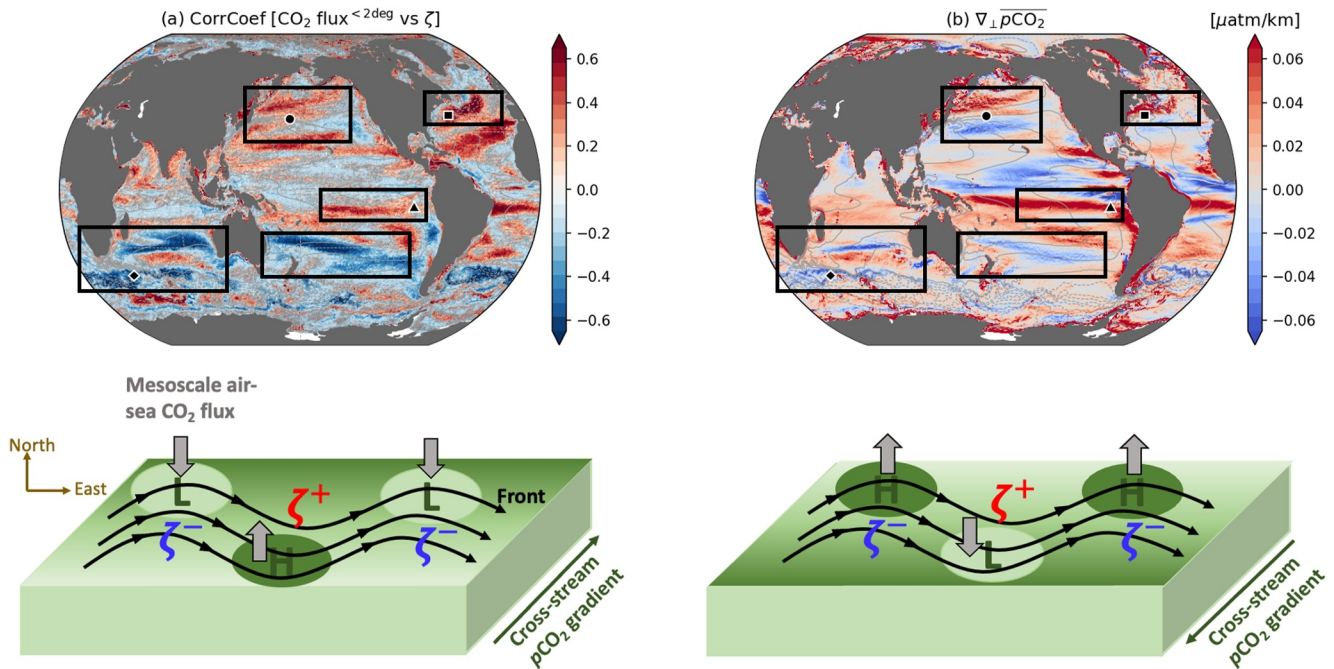


Figure 5. (a) Global distribution of correlation coefficients between monthly mesoscale-related CO₂ flux and relative vorticity (gray areas indicate locations that are not statistically significant at the 90% significance level); (b) Global mean cross-stream pCO₂ gradient; black markers are the four locations analyzed in Figure 3 and black boxes denote select regions with high mesoscale activity and CO₂ flux variance (Figure 2b); (c) Schematic diagram illustrating a scenario with positive correlation between relative vorticity and mesoscale-related CO₂ flux; (d) same as (c) but for a negative correlation.

the Antarctic Circumpolar Current, and the equatorial Pacific. The local distribution of cumulative $F_{\text{CO}_2}^{<2^\circ}$ displays zonal bands alternating between positive (a net source) and negative (a net sink) due to the meandering nature of ocean mesoscale currents. We further show that $F_{\text{CO}_2}^{<2^\circ}$ is strongly linked to relative vorticity and the background cross-stream $p\text{CO}_2$ gradient. With the presence of a positive cross-stream gradient of $p\text{CO}_2$, $F_{\text{CO}_2}^{<2^\circ}$ is positively correlated with local relative vorticity, where mesoscale motions with negative vorticity tend to lower local $p\text{CO}_2$ and lead to CO₂ uptake, and vice versa for positive vorticity. In the scenario with a negative cross-stream gradient of $p\text{CO}_2$, $F_{\text{CO}_2}^{<2^\circ}$ and relative vorticity are negatively correlated.

As one of the most common features of the ocean mesoscale, coherent eddies comprise a significant portion of ocean transient energy (Martínez-Moreno et al., 2019). Ford et al. (2023) estimated eddy-induced modulations of air-sea CO₂ flux in the South Atlantic Ocean using in-situ observations and a Lagrangian eddy atlas product, finding that regional long-lived eddies can contribute to carbon uptake of 0.06 MtC per year. The mesoscale-associated CO₂ flux, $F_{\text{CO}_2}^{<2^\circ}$, analyzed here includes the contribution from coherent eddies. For a similar region of the South Atlantic, $F_{\text{CO}_2}^{<2^\circ}$ in POP-BGC-HR indicates a mean carbon sink of 0.04 MtC per year, of similar magnitude to observations by Ford et al. (2023) based on 67 long-lived eddy samples in the South Atlantic. Note, however, that in our analysis, $F_{\text{CO}_2}^{<2^\circ}$ includes not only the large-scale eddies, but also smaller-scale features. Although large coherent eddies have been shown to dominate mesoscale-related CO₂ fluxes in the South Atlantic (T. Smith et al., 2023), the smaller-scale features may contribute some net source/sink not accounted for in Ford et al. (2023) analysis. Although the overall magnitude of the globally integrated net mesoscale-related CO₂ uptake is small (on the order of 10⁵ tC per year) in comparison to the ocean's total capacity for carbon absorption (of order 10³ MtC per year), mesoscale processes may still exert a significant influence on the ocean carbon budget. For example, features at this scale induce isopycnal mixing (Gnanadesikan et al., 2015) and modulate mixed layer depth (Gaube et al., 2019), likely leading to variations in ocean surface $p\text{CO}_2$ (Prend et al., 2022) and affecting the supply of nutrients being entrained from subsurface waters; they can alter wind speed (therefore gas transfer velocity at the air-sea interface) by modifying the atmospheric boundary layer (Small et al., 2008), and influence local carbon export (Harrison et al., 2018).

Simulated variations in air-sea CO₂ flux from the Coupled Model Intercomparison Project version 5 (CMIP5) low-resolution (not eddy-resolving) ocean models exhibit large biases (Mongwe et al., 2018). A better representation of mesoscale flows in models is essential for reliably simulating the carbon cycle and predicting its response to different climate forcings (Gnanadesikan et al., 2015). The analysis of mesoscale-related CO₂ flux presented here is based on resultant biogeochemical fields from an eddy-resolving simulation, wherein the influence of mesoscale processes is already incorporated into the simulated carbon budget. It is likely that the complete influence of mesoscale flows on the CO₂ flux field is not fully isolated through the coarse-graining applied here. Future work involving a comparison of mesoscale-related CO₂ flux between low- and high-resolution coupled simulations is necessary. In this study, we have considered only the overall influence of mesoscale motions on CO₂ flux variability and have not partitioned the influence into physical and biological drivers. An examination of different physical/biogeochemical drivers for shaping ocean pCO₂ variations associated with mesoscale activity is a subject for future research. Furthermore, submesoscale flows in the ocean, not considered in this study, have the potential to enhance mesoscale tracer transport through an inverse energy cascade (Zhang et al., 2023). Their contribution to mesoscale-related CO₂ flux needs to be evaluated in future research.

There is some evidence for enhanced mesoscale energy (Beech et al., 2022; Martínez-Moreno et al., 2021) and associated tracer transport (Guo, Bachman, et al., 2022) under global warming, suggesting a potentially larger role for mesoscale phenomena in future air-sea carbon exchange. In some parts of the global oceans, variations in pCO₂, which directly affect changes in air-sea CO₂ flux, are predominantly influenced by temperature changes (Guo & Timmermans, 2024b; Takahashi et al., 2002). Considering the context of strengthened temperature variance (Guo, Bachman, et al., 2022) and more frequent and extreme marine heatwaves (Frölicher et al., 2018) in recent decades, the thermal component of pCO₂ variations is likely undergoing modifications as a consequence, potentially altering mesoscale-induced CO₂ exchange. The strong links between mesoscale motions and ocean carbon cycling underscores the need for an expanded observational network to better monitor ocean carbon parameters and model development to resolve small-scale ocean features in the face of a changing climate. Improved understanding of the mechanisms through which mesoscale phenomena may affect the broader carbon cycle is essential for reliable climate projections and the development of effective ocean-based strategies for mitigating the impacts of climate change.

Data Availability Statement

The sea surface pCO₂ and air-sea CO₂ flux data set is available in (Jersild et al., 2023). The sea surface height data are available in (CMEMS, 2023). Model data used in this work can be found in (Guo & Timmermans, 2024a).

Acknowledgments

Support for this research was provided by the Yale Center for Natural Carbon Capture. We thank the editor and two anonymous reviewers for comments that greatly improved the quality of this paper. We thank Matthew Long, Frank Bryan, Keith Lindsay, Kristen Krumhardt, and Michael Levy from National Center for Atmospheric Research for providing access to the POP-BGC-HR simulation. We would like to acknowledge high-performance computing support from Cheyenne and Casper supercomputers provided by NCAR's Computational and Information Systems Laboratory, sponsored by the National Science Foundation.

References

- Aluie, H., Hecht, M., & Vallis, G. K. (2018). Mapping the energy cascade in the North Atlantic Ocean: The coarse-graining approach. *Journal of Physical Oceanography*, 48(2), 225–244. <https://doi.org/10.1175/jpo-d-17-0100.1>
- Arroyo, M., Shadwick, E., & Tilbrook, B. (2019). Summer carbonate chemistry in the Dalton Polynya, east Antarctica. *Journal of Geophysical Research: Oceans*, 124(8), 5634–5653. <https://doi.org/10.1029/2018jc014882>
- Beech, N., Rackow, T., Semmler, T., Danilov, S., Wang, Q., & Jung, T. (2022). Long-term evolution of ocean eddy activity in a warming world. *Nature Climate Change*, 12(10), 910–917. <https://doi.org/10.1038/s41558-022-01478-3>
- Bryan, F., & Bachman, S. (2015). Isohaline salinity budget of the North Atlantic salinity maximum. *Journal of Physical Oceanography*, 45(3), 724–736. <https://doi.org/10.1175/jpo-d-14-0172.1>
- Chelton, D. B., DeSzoeke, R. A., Schlax, M. G., El Naggar, K., & Siwertz, N. (1998). Geographical variability of the first baroclinic Rossby radius of deformation. *Journal of Physical Oceanography*, 28(3), 433–460. [https://doi.org/10.1175/1520-0485\(1998\)028<0433:gvotfb>2.0.co;2](https://doi.org/10.1175/1520-0485(1998)028<0433:gvotfb>2.0.co;2)
- Chelton, D. B., Schlax, M. G., & Samelson, R. M. (2011). Global observations of nonlinear mesoscale eddies. *Progress in Oceanography*, 91(2), 167–216. <https://doi.org/10.1016/j.pocean.2011.01.002>
- Chen, F., Cai, W.-J., Benitez-Nelson, C., & Wang, Y. (2007). Sea surface pCO₂-SST relationships across a cold-core cyclonic eddy: Implications for understanding regional variability and air-sea gas exchange. *Geophysical Research Letters*, 34(10). <https://doi.org/10.1029/2006gl028058>
- CMEMS. (2023). Global Ocean gridded L 4 sea surface heights and derived variables reprocessed 1993 ongoing. E.U. Copernicus marine service information (CMEMS). [Dataset]. *Marine Data Store (MDS)*. <https://doi.org/10.48670/moi-00148>
- Ford, D. J., Tilstone, G. H., Shutler, J. D., Kitidis, V., Sheen, K. L., Dall'Olmo, G., & Orselli, I. B. (2023). Mesoscale eddies enhance the air-sea CO₂ sink in the South Atlantic Ocean. *Geophysical Research Letters*, 50(9), e2022GL102137. <https://doi.org/10.1029/2022gl102137>
- Frenger, I., Gruber, N., Knutti, R., & Münnich, M. (2013). Imprint of Southern Ocean eddies on winds, clouds and rainfall. *Nature Geoscience*, 6(8), 608–612. <https://doi.org/10.1038/ngeo1863>
- Friedlingstein, P., O'sullivan, M., Jones, M. W., Andrew, R. M., Bakker, D. C., Hauck, J., et al. (2023). Global carbon budget 2023. *Earth System Science Data*, 15(12), 5301–5369. <https://doi.org/10.5194/essd-15-5301-2023>
- Frölicher, T. L., Fischer, E. M., & Gruber, N. (2018). Marine heatwaves under global warming. *Nature*, 560(7718), 360–364. <https://doi.org/10.1038/s41586-018-0383-9>
- Gaube, P., McGillicuddy, D. J., Jr., & Moulin, A. J. (2019). Mesoscale eddies modulate mixed layer depth globally. *Geophysical Research Letters*, 46(3), 1505–1512. <https://doi.org/10.1029/2018gl080006>

- Gnanadesikan, A., Pradal, M.-A., & Abernathy, R. (2015). Isopycnal mixing by mesoscale eddies significantly impacts oceanic anthropogenic carbon uptake. *Geophysical Research Letters*, 42(11), 4249–4255. <https://doi.org/10.1002/2015gl064100>
- Gruber, N., Bakker, D. C., DeVries, T., Gregor, L., Hauck, J., Landschützer, P., et al. (2023). Trends and variability in the ocean carbon sink. *Nature Reviews Earth & Environment*, 4(2), 119–134. <https://doi.org/10.1038/s43017-022-00381-x>
- Gu, Y., Katul, G. G., & Cassar, N. (2023). Multiscale temporal variability of the global air-sea CO₂ flux anomaly. *Journal of Geophysical Research: Biogeosciences*, 128(6), e2022JG006934. <https://doi.org/10.1029/2022jg006934>
- Guo, Y., Bachman, S., Bryan, F., & Bishop, S. (2022). Increasing trends in oceanic surface poleward eddy heat flux observed over the past three decades. *Geophysical Research Letters*, 49(16), e2022GL099362. <https://doi.org/10.1029/2022gl099362>
- Guo, Y., Bishop, S., Bryan, F., & Bachman, S. (2022). A global diagnosis of eddy potential energy budget in an eddy-permitting ocean model. *Journal of Physical Oceanography*, 52(8), 1731–1748. <https://doi.org/10.1175/jpo-d-22-0029.1>
- Guo, Y., Bishop, S., Bryan, F., & Bachman, S. (2023). Mesoscale variability linked to interannual displacement of Gulf Stream. *Geophysical Research Letters*, 50(7), e2022GL102549. <https://doi.org/10.1029/2022gl102549>
- Guo, Y., & Bishop, S. P. (2022). Surface divergent eddy heat fluxes and their impacts on mixed layer eddy-mean flow interactions. *Journal of Advances in Modeling Earth Systems*, 14(4), e2021MS002863. <https://doi.org/10.1029/2021ms002863>
- Guo, Y., & Timmermans, M.-L. (2024a). Data for “The role of ocean mesoscale variability in air-sea CO₂ exchange: A global perspective” [Dataset]. *Zenodo*. <https://doi.org/10.5281/zenodo.10988867>
- Guo, Y., & Timmermans, M.-L. (2024b). Global ocean pCO₂ variation regimes: Spatial patterns and the emergence of a hybrid regime. *Journal of Geophysical Research: Oceans*. in press. <https://doi.org/10.1029/2023JC020679>
- Harrison, C. S., Long, M. C., Lovenduski, N. S., & Moore, J. K. (2018). Mesoscale effects on carbon export: A global perspective. *Global Biogeochemical Cycles*, 32(4), 680–703. <https://doi.org/10.1002/2017gb005751>
- Hunke, E. C., Lipscomb, W. H., Turner, A. K., Jeffery, N., & Elliott, S. (2010). *Cice: The los alamos sea ice model documentation and software user's manual version 4.1 la-cc-06-012. T-3 Fluid Dynamics Group* (Vol. 675, p. 500). Los Alamos National Laboratory.
- Jersild, A., Landschützer, P., Gruber, N., & Bakker, D. C. E. (2023). An observation-based global monthly gridded sea surface pCO₂ and air-sea CO₂ flux product from 1982 onward and its monthly climatology (NCEI Accession 0160558) [Dataset]. NOAA National Centers for Environmental Information. <https://doi.org/10.7289/V5Z899N6>
- Jones, E. M., Hoppema, M., Strass, V., Hauck, J., Salt, L., Ossebaar, S., et al. (2017). Mesoscale features create hotspots of carbon uptake in the Antarctic Circumpolar Current. *Deep Sea Research Part II: Topical Studies in Oceanography*, 138, 39–51. <https://doi.org/10.1016/j.dsr2.2015.10.006>
- Kim, D., Lee, S.-E., Cho, S., Kang, D.-J., Park, G.-H., & Kang, S. K. (2022). Mesoscale eddy effects on sea-air CO₂ fluxes in the northern philippinsea. *Frontiers in Marine Science*, 9, 970678. <https://doi.org/10.3389/fmars.2022.970678>
- Kobayashi, S., Ota, Y., Harada, Y., Ebata, A., Moriya, M., Onoda, H., et al. (2015). The JRA-55 reanalysis: General specifications and basic characteristics. *Journal of the Meteorological Society of Japan. Ser. II*, 93(1), 5–48. <https://doi.org/10.2151/jmsj.2015-001>
- Landschützer, P., Gruber, N., & Bakker, D. (2020). An observation-based global monthly gridded sea surface pCO₂ and air-sea CO₂ flux product from 1982 onward and its monthly climatology. NCEI Accession.160558.
- Landschützer, P., Gruber, N., & Bakker, D. C. (2016). Decadal variations and trends of the global ocean carbon sink. *Global Biogeochemical Cycles*, 30(10), 1396–1417. <https://doi.org/10.1002/2015gb005359>
- Long, M. C., Moore, J. K., Lindsay, K., Levy, M., Doney, S. C., Luo, J. Y., et al. (2021). Simulations with the marine biogeochemistry library (MARBL). *Journal of Advances in Modeling Earth Systems*, 13(12), e2021MS002647. <https://doi.org/10.1029/2021ms002647>
- Martínez-Moreno, J., Hogg, A. M., England, M. H., Constantinou, N. C., Kiss, A. E., & Morrison, A. K. (2021). Global changes in oceanic mesoscale currents over the satellite altimetry record. *Nature Climate Change*, 11(5), 397–403. <https://doi.org/10.1038/s41558-021-01006-9>
- Martínez-Moreno, J., Hogg, A. M., Kiss, A. E., Constantinou, N. C., & Morrison, A. K. (2019). Kinetic energy of eddy-like features from sea surface altimetry. *Journal of Advances in Modeling Earth Systems*, 11(10), 3090–3105. <https://doi.org/10.1029/2019ms001769>
- Melnichenko, O., Hacker, P., & Müller, V. (2021). Observations of mesoscale eddies in satellite SSS and inferred eddy salt transport. *Remote Sensing*, 13(2), 315. <https://doi.org/10.3390/rs13020315>
- Miller, S. D., Emond, M., Vandemark, D., Shellito, S., Covert, J., Bogoev, I., & Swiatek, E. (2024). Field evaluation of an autonomous, low-power eddy covariance CO₂ flux system for the marine environment. *Journal of Atmospheric and Oceanic Technology*, 41(3), 279–293. <https://doi.org/10.1175/jtech-d-23-0076.1>
- Miller, S. D., Marandino, C., & Saltzman, E. S. (2010). Ship-based measurement of air-sea CO₂ exchange by eddy covariance. *Journal of Geophysical Research*, 115(D2). <https://doi.org/10.1029/2009jd012193>
- Mongwe, N. P., Vichi, M., & Monteiro, P. M. (2018). The seasonal cycle of pCO₂ and CO₂ fluxes in the Southern Ocean: Diagnosing anomalies in CMIP5 Earth system models. *Biogeosciences*, 15(9), 2851–2872. <https://doi.org/10.5194/bg-15-2851-2018>
- Persch, C. F., DiNezio, P., & Lovenduski, N. S. (2023). The impact of orbital precession on air-sea CO₂ exchange in the Southern Ocean. *Geophysical Research Letters*, 50(21), e2023GL103820. <https://doi.org/10.1029/2023gl103820>
- Pezzi, L. P., de Souza, R. B., Santini, M. F., Miller, A. J., Carvalho, J. T., Parise, C. K., et al. (2021). Oceanic eddy-induced modifications to air-sea heat and CO₂ fluxes in the Brazil – malvinasconfluence. *Scientific Reports*, 11(1), 10648. <https://doi.org/10.1038/s41598-021-89985-9>
- Prend, C. J., Hunt, J. M., Mazloff, M. R., Gille, S. T., & Talley, L. D. (2022). Controls on the boundary between thermally and non-thermally driven pCO₂ regimes in the South Pacific. *Geophysical Research Letters*, 49(9), e2021GL095797. <https://doi.org/10.1029/2021gl095797>
- Small, R. d., deSzoeko, S. P., Xie, S., O'Neill, L., Seo, H., Song, Q., et al. (2008). Air-sea interaction over ocean fronts and eddies. *Dynamics of Atmospheres and Oceans*, 45(3–4), 274–319. <https://doi.org/10.1016/j.dynatmoce.2008.01.001>
- Smith, R., Jones, P., Briegleb, B., Bryan, F., Danabasoglu, G., Dennis, J., et al. (2010). The parallel ocean program (POP) reference manual ocean component of the community climate system model (CCSM) and community earth system model (CESM). *LAUR-01853*, 141, 1–140.
- Smith, T., Nicholson, S.-A., Engelbrecht, F., Chang, N., Mongwe, N., & Monteiro, P. (2023). The heat and carbon characteristics of modeled mesoscale eddies in the South-East Atlantic Ocean. *Journal of Geophysical Research: Oceans*, 128(12), e2023JC020337. <https://doi.org/10.1029/2023jc020337>
- Storer, B. A., & Aluie, H. (2023). FlowSieve: A coarse-graining utility for geophysical flows on the sphere. *Journal of Open Source Software*, 8(84), 4277. <https://doi.org/10.21105/joss.04277>
- Takahashi, T., Sutherland, S. C., Sweeney, C., Poisson, A., Metzl, N., Tilbrook, B., et al. (2002). Global sea-air CO₂ flux based on climatological surface ocean pCO₂, and seasonal biological and temperature effects. *Deep Sea Research Part II: Topical Studies in Oceanography*, 49(9–10), 1601–1622. [https://doi.org/10.1016/s0967-0645\(02\)00003-6](https://doi.org/10.1016/s0967-0645(02)00003-6)
- Takahashi, T., Sutherland, S. C., Wanninkhof, R., Sweeney, C., Feely, R. A., Chipman, D. W., et al. (2009). Climatological mean and decadal change in surface ocean pCO₂, and net sea-air CO₂ flux over the global oceans. *Deep Sea Research Part II: Topical Studies in Oceanography*, 56(8–10), 554–577. <https://doi.org/10.1016/j.dsr2.2008.12.009>

- Tokoro, T., Nakaoka, S., Takao, S., Saito, S., Sasano, D., Enyo, K., et al. (2023). Statistical analysis of spatiotemporal variations of air-sea CO₂ fluxes in the Kuroshio region. *Journal of Geophysical Research: Oceans*, *128*(11), e2023JC019762. <https://doi.org/10.1029/2023jc019762>
- Tozawa, M., Nomura, D., Nakaoka, S.-i., Kiuchi, M., Yamazaki, K., Hirano, D., et al. (2022). Seasonal variations and drivers of surface ocean pCO₂ in the seasonal ice zone of the eastern Indian sector, Southern Ocean. *Journal of Geophysical Research: Oceans*, *127*(1), e2021JC017953. <https://doi.org/10.1029/2021jc017953>
- Wanninkhof, R. (2014). Relationship between wind speed and gas exchange over the ocean revisited. *Limnology and Oceanography: Methods*, *12*(6), 351–362. <https://doi.org/10.4319/lom.2014.12.351>
- Wong, S. C., McKinley, G. A., & Seager, R. (2022). Equatorial Pacific pCO₂ interannual variability in CMIP6 models. *Journal of Geophysical Research: Biogeosciences*, *127*(12), e2022JG007243. <https://doi.org/10.1029/2022jg007243>
- Zhang, Z., Liu, Y., Qiu, B., Luo, Y., Cai, W., Yuan, Q., et al. (2023). Submesoscale inverse energy cascade enhances Southern Ocean eddy heat transport. *Nature Communications*, *14*(1), 1335. <https://doi.org/10.1038/s41467-023-36991-2>
- Zhang, Z., Wang, W., & Qiu, B. (2014). Oceanic mass transport by mesoscale eddies. *Science*, *345*(6194), 322–324. <https://doi.org/10.1126/science.1252418>